EUROPHYSICS LETTERS 1 September 2003

Europhys. Lett., **63** (5), pp. 771–777 (2003)

Overdamped interlayer exchange coupling and disorder-dominated magnetoresistance in $La_{0.7}Ca_{0.3}MnO_3/LaNiO_3$ superlattices

P. Padhan[1], R. C. Budhani[1] and R. P. S. M. Lobo[2]

[1] *Department of Physics, Indian Institute of Technology - Kanpur, 208016, India*

[2] *Laboratoire de Physique du Solide, Ecole Supérieure de Physique, Chimie Industrielles de la Ville de Paris, CNRS UPR 5 - 75231 Paris, Cedex 5, France*

(received 14 January 2003; accepted in final form 20 June 2003)

PACS. 75.70.Cn – Magnetic properties of interfaces (multilayers, superlattices, heterostructures).

PACS. 75.47.Gk – Colossal magnetoresistance.

PACS. 75.47.Lx – Manganites.

Abstract. – Magnetization and magnetoresistance (MR) measurements are reported on superlattices consisting of alternate layers of 20 unit cell (u.c.) thick $La_{0.7}Ca_{0.3}MnO_3$ (LCMO) and n u.c. $LaNiO_3$ (LNO), where n varies from 1 to 10. The saturation field (H_s) and remnant magnetization (M_r) show antiferromagnetic (AF) interlayer coupling for $n \leq 2$ followed by an overdamped oscillatory behavior with a period of ≈ 4 u.c. with the increasing n. The low-temperature MR of the AF-coupled superlattices is characterized by a steep increase up to a critical field $H_s{}^*$ ($\approx H_s$) followed by a $\sim H^\alpha$ ($\alpha < 1.0$) dependence, whereas in the ferromagnetically coupled samples the MR rises monotonically as $\sim H^\alpha$ with no $H_s{}^*$. We attribute the overdamped oscillations in M_r and H_s, and the dual nature of MR to disorder modified quantum interference in the spacer layers.

Interlayer exchange coupling (IEC) and its oscillatory nature in 3d transition-metal–based magnetic multilayers have been studied extensively in the last decade [1, 2]. In the systems where magnetic layers of Fe, Co or Ni are separated by a non-magnetic simple metal, it is generally recognized that the IEC interaction is carried by the conduction electrons of the latter [3, 4]. The strength and range of this interaction depend sensitively on the effects of scattering of charge carriers by disorder in the spacer layer and at the spacer-ferromagnet interfaces. In the backdrop of these findings, the recent discovery of overdamped oscillations in IEC of certain multilayers [5, 6] where the constituents are compounds with inherent complexities of narrow bands, short mean free path and electron correlations is quite fascinating.

The nature of IEC in 3d transition-metal–based superlattices is clearly linked with the behavior of magnetoresistance (MR). The MR also shows oscillations with the increasing spacer layer thickness and its period matches with the period of the IEC [7]. A large negative MR when IEC is antiferromagnetic indicates ease in spin diffusion through the spacer as magnetization vectors of the neighboring ferromagnetic layers are made parallel by the external magnetic field. However, limited transport measurements on superlattices made of compounds show no such correlation between the MR and IEC.

In this letter we report extensive measurements of the interlayer exchange coupling and Current-in-Plane (CIP) magnetoresistance in superlattices of the ferromagnetic manganite $La_{0.7}Ca_{0.3}MnO_3$ (LCMO) and a Pauli paramagnet $LaNiO_3$ (LNO), which remains metallic

down to 4.2 K. While the saturation field (H_s) and remnant magnetization (M_r) of these superlattices show an overdamped oscillatory behavior with increasing LNO layer thickness, the magnetoresistance reveals a remarkable dual character. The MR derives contributions from the ease in carrier transmission across interfaces as the magnetization of the adjacent LCMO layers becomes parallel with the field. This effect saturates at $\sim H_s$. The second contribution to MR, which is additive, seems to come from field-assisted hopping of carriers between localized moments at the interfaces. The manifestations of interfacial disorder in these superlattices are seen in their resistivity as well. The measured resistivity of these periodic structures is much higher than the resistivity inferred from a simple parallel-resistor network calculation using bulk resistivities of LCMO and LNO [8]. Since this feature is universally seen in manganites [9–15] and high-T_c–based superlattices irrespective of the process used for synthesis [15, 16], we argue that the role of interfaces needs to be addressed adequately while discussing magnetotransport in oxide-based superlattices.

A multitarget pulsed-laser deposition system has been used for growth of LCMO and LNO thin films and LCMO/LNO superlattices on (001) $LaAlO_3$ (LAO) substrates. The lattice parameter of cubic LAO ($a_{LAO} = 3.792$ Å) provides low lattice mismatch for epitaxial growth of LCMO and LNO whose lattice parameters are $a_{LCMO} = 3.86$ Å and $a_{LNO} = 3.83$ Å, respectively. However, because of the non-zero difference between the lattice parameters, some degree of compressive strain is expected in these superlattices [8]. The other commonly used substrate for epitaxial growth of manganite films is (001) $SrTiO_3$, whose lattice parameter of 3.905 Å would lead to a tensile strain in LCMO and LNO films. While (110) cut $NdGaO_3$ ($a = 3.86$ Å) provides the least lattice mismatch, the excessive cost of these substrates is a limitation. The optimized deposition conditions such as temperature, oxygen partial pressure and growth rate are reported elsewhere [8, 17]. The superlattice structures were synthesized by repeating 15 times the bilayers composed of 20 unit cells (u.c.) LCMO and n u.c. LNO with n taking values from 1 to 10. These periodic modulations in the composition of the film created on the basis of an established deposition rate of LCMO and LNO were confirmed by the positions of superlattice reflections in X-ray θ-2θ scans. The X-ray diffraction measurements also revealed exclusive (001)-oriented growth of the multilayers. We have used a superconducting quantum interference device based magnetometer (Quantum Design MPMS-5) for magnetization measurements. Two sets of magnetization data were taken with field in (100) and (010) directions on the plane of the multilayer. The results were identical within the accuracy of measurements of the MPMS-5 system ($\approx 1.5\%$), indicating the absence of any in-plane anisotropy along the two orientations. Here we also report temperature and field scans of current-in-plane magnetoresistance taken in a variable-temperature cryostat equipped with a 4 tesla superconducting solenoid.

Magnetization isothermal measurement as a function of applied field (H) is the commonly used method to establish the nature of interlayer coupling. In fig. 1 we show M *vs.* H data of the multilayers taken at 10 K. The magnetic field in these measurements was aligned parallel to the (100) axis of the substrate. For the sake of clarity, data for only a selected number of superlattices are shown and the magnetization has been normalized with respect to its saturation value. M_s and H_s have been extracted from the point on the M-H loops at which dM/dH becomes zero, after taking into account the weakly diamagnetic response of the substrate. The large saturation field and negligible remnant magnetization (M_r) seen in the case of samples with 1 and 2 u.c. thick LNO spacer are indicative of antiferromagnetic exchange coupling between the LCMO layers. The saturation field drops when the LNO thickness is increased to 3 unit cells and remains low for the higher values of n. The saturation field and remnant magnetization for all multilayers are shown in fig. 2. The variation of H_s with the spacer layer thickness shows a peak at $n \approx 2$ followed by a minimum at $n \approx 4$ and then a

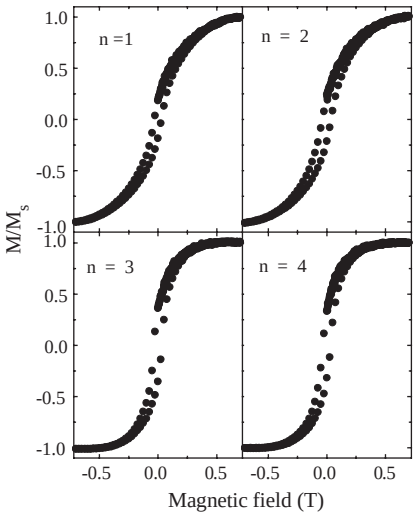

Fig. 1

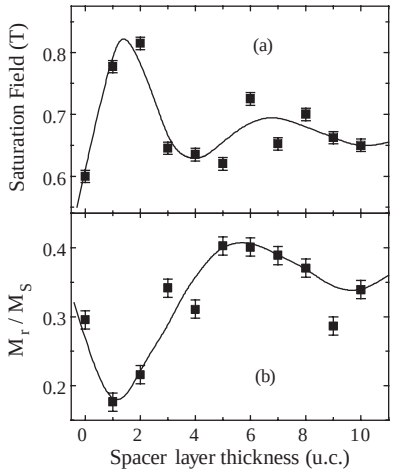

Fig. 2

Fig. 1 – Normalized magnetic moment (M/M_s) of LCMO/LNO superlattices at 10 K plotted as a function of applied magnetic field. Data for samples with LNO layer thickness of 1, 2, 3 and 4 u.c. are shown.

Fig. 2 – Panel (a) shows the variation of the saturation field H_s with LNO spacer layer thickness. The ratio of the remnant and saturation moments (M_r/M_s) for different superlattices is shown in the lower panel (b). Solid lines in the figure are a guide to the eye. Error bars in panels (a) and (b) reflect the field step size used in the measurement of M *vs.* H, and the standard deviation in the measurement of moment by the MPMS-5 system, respectively. All data were taken at 10 K.

second broad peak of much lower intensity centered at $n \approx 7$. The remnant magnetization, on the other hand, rises rapidly between $n = 2$ and $n = 4$, reaches a peak value at $n = 6$ and then drops on a further increase in n.

It is instructive to compare the behavior of H_s seen in fig. 2 with the data on superlattices of pure metals and compounds. In the case of Fe/Cr, the canonical GMR superlattice for example, a distinct peak is seen in H_s at Cr spacer thickness (d_s) of $\sim$ 10 Å followed by a second peak and a third-peak–like feature at 25 Å and 45 Å, respectively [1]. A similar period has been observed in Fe_3O_4/TiN with much stronger damping of the oscillations at the higher TiN spacer thickness [5]. In the case of $La_{2/3}Ba_{1/3}MnO_3/LaNiO_3$ (LBMO/LNO) superlattices, however, a fully developed ferromagnetic coupling is seen for 5 u.c. thick LNO [6]. While this number exceeds our value by $\sim$ 1 u.c. of LNO, the overall features of the data shown in fig. 2(a) are similar to what has been observed in the case of LBMO/LNO multilayers. Bruno and Cheppert [4] have shown that in the framework of the Ruderman-Kittel-Kasuya-Yoshida (RKKY) exchange coupling, the period of oscillations depends on the Fermi surface parameters of the spacer layer. Since the spacer layers are identical in the two cases, the subtle difference in the position of the first minimum is perhaps due to the difference in the thickness of the ferromagnetic layers, as suggested by Barnas [18] for metallic superlattices. The behavior of remnant magnetization with increasing d_s, as shown in fig. 2(b), is consistent with the picture of a changeover from antiferromagnetic-to-ferromagnetic coupling between the LCMO layers. The large value of M_r ($\sim$ 35% of M_s) for $d_s > 3$ u.c. reflects the squareness of the hysteresis loop typical of a soft ferromagnet.

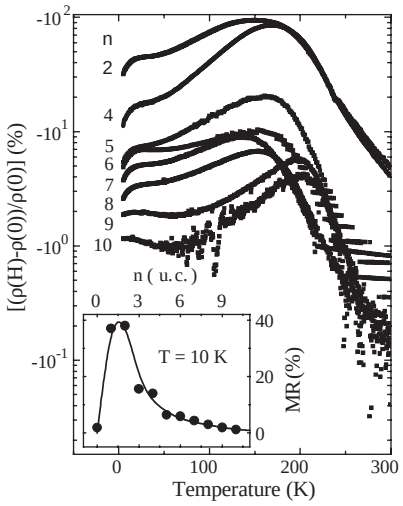

Fig. 3

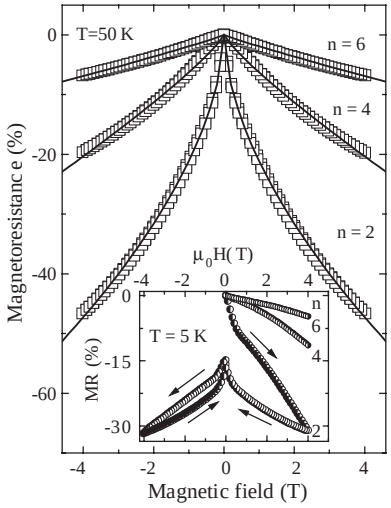

Fig. 4

Fig. 3 – Current-in-plane magnetoresistance of several superlattices measured at 4 tesla as a function of temperature, with the field aligned in a Lorentz force free configuration. Magnetoresistance drops precipitously as the thickness of LNO layers is increased (note the logarithmic scale). Also at $T < 20\,\mathrm{K}$ a drop in MR is prominent in samples with thinner LNO layers. The inset shows the MR of different superlattices at 10 K.

Fig. 4 – Magnetic-field dependence of MR at 50 K for three superlattices with $n = 2$, 4 and 6. Data for a complete field cycle between +4 and −4 tesla are shown. The MR at 50 K is completely reversible. Solid lines in the figure are fits of the type $\mathrm{MR} \sim H^{\alpha}$. The inset shows a complete loop of MR at 5 K for the sample with $n = 2$. The critical field $H_s{}^*$ is marked in the figure. The inset also shows MR of the $n = 4$ and $n = 6$ samples as the field is increased from zero to 4 tesla.

The nature of coupling between the ferromagnetic layers is expected to have a distinct bearing on the magnetoresistance of the superlattices. In fig. 3 we show the MR $[(\rho(H,T) - \rho(0,T))/\rho(0,T)]$ at 4 tesla of a large number of LCMO/LNO samples in the temperature range between 4.2 K and 300 K. For all samples, the MR rises gradually on cooling below 300 K, reaches a peak value in the vicinity of the Curie temperature and then drops on further cooling. However, there are many interesting features beneath this broad description of the MR. For example, i) The MR of samples with thin spacer (≤ 2 u.c.) is ≈ 100 percent near T_c and it stays high on lowering the temperature. T_c has been identified with the temperature where zero-field resistivity has the peak and it compares well with the T_c deduced from field-cooled magnetization measurements. ii) While the T_c of thick (> 400 Å) LCMO film and LCMO/LNO with $n > 8$ u.c. is ≈ 220 K, a significant drop in the Curie temperature is seen at the lower values of n. iii) As shown in the inset of fig. 3, the MR at 10 K has a peak at $n = 2$ followed by a rapid drop with increasing n. iv) The resistivity of all the samples at $T < T_c$ was metallic but for a $\log(1/T)$ divergence at the lowest temperature for the sample with $n \leq 8$. v) In the regime of temperature where $\rho \sim \log(1/T)$, the MR drops precipitously on lowering the temperature.

In order to address the question whether the MR is a consequence of the ease in transport of spin-polarized carriers across the spacer as the moments of the FM layers become parallel, in fig. 4 we show field scans of MR for samples with $n = 2$, 4 and 6. At 50 K, the magnetoresistance of all three samples is negative even at the lowest field and its magnitude continues to increase with the field according to a dependence of the type $\mathrm{MR} \sim H^{\alpha}$ with $\alpha = 0.6$, 0.85

and 0.92 for $n = 2$, 4 and 6, respectively. The magnetoresistance is also fully reversible at this temperature. A strikingly different behavior of MR is seen at 5 K for the sample with $n = 2$, for which the H_s data suggest antiparallel magnetic coupling between the LCMO layers. As seen in the inset of fig. 4, the MR first changes rapidly with the field till 0.8 tesla followed by a much slower change. This characteristic field $H_s{}^*$ is same as the saturation field shown in figs. 1 and 2. In the inset of fig. 4 we also show the field increasing branch of the MR curve for the $n = 4$ and $n = 6$ samples. Here the magnetoresistance increases smoothly with the field without any signatures of an $H_s{}^*$. Note that the LCMO layers in these samples are FM coupled. The marked change in the behavior of magnetoresistance with the increasing field strongly suggests a correlation between MR and the magnetic coupling of the sample with $n = 2$. Another interesting feature of the magnetoresistance at low temperatures (< 20 K) is a pronounced hysteresis as seen in the inset for the sample with $n = 2$. Similar irreversibility is also present in MR *vs.* H loops of other samples (not shown for the sake of clarity). From the data of figs. 1, 2, 3 and 4 it is clear that unlike the case of most of the 3d-transition-metal–based superlattices, a direct and distinct correlation between saturation of MR and H_s does not exist in the present case. This is barring the characteristic field $H_s{}^*$ seen in the MR of the antiferromagnetically coupled $n = 2$ superlattices.

In metallic superlattices, a correlation between AF interlayer exchange coupling and large negative magnetoresistance depends on the extent of interfacial disorder. For example in Fe-Nb multilayers [19], while H_s and M_r oscillate with increasing Nb layer thickness, the MR remains small even in the case of the AF coupled samples. Similarly, non-magnetic impurities at interface seem to suppress MR without changing the AF coupling [20]. Electron transport and magnetic properties of transition metal oxides are likely to be much more susceptible to interfaces and interfacial disorder due to the covalency of the bonds. Even at a defect-free interface, the truncation of the 3-dimensional environment of the Mn and Ni ions in the bulk LCMO and LNO, respectively, can lead to different site spins and overlap integrals for charge transport. The possibilities of alloying through the formation of the compound $La_xNi_{1-x}MnO_3$ and the lattice-mismatch–related strain add to this problem. In our earlier studies of transport in ultrathin films of LCMO, LNO and $(LCMO)_m/(LNO)_n$ superlattices ($m = 10$ u.c. and n variable), we have seen clear signatures of a 3–4 u.c. thick disordered interfacial phase (DIP) [8]. Our magnetization measurements also attest to this picture. In fig. 5 we show the variation of saturation magnetization in units of Bohr magneton (μ_B) per Mn ion with the LNO layer thickness. The error bars in the figure reflect the uncertainty in the measurements of sample area, which was different for each sample. A simple counting of Mn^{4+} and Mn^{3+} spins in the bulk $La_{0.7}Ca_{0.3}MnO_3$ yields an average moment of 3.7 μ_B per Mn site. Measurements of magnetization on a 1000 Å film of LCMO are consistent with this number. In the multilayers with lower LNO spacer layer thickness, the magnetic moment per Mn ion shows a small but distinct drop. We also observe a similar drop in the Curie temperature. However, as n increases beyond 6, the M_s and T_c show a steady increase and for the superlattice with $n = 10$, both these quantities approach the bulk value. In the inset of fig. 5 we show typical zero-field–cooled (ZFC) and field-cooled (FC) magnetization curves taken at 10 K for the $n = 4$ multilayer. The ZFC and FC magnetization at lower temperatures have a large difference, clearly suggesting some kind of freezing/frustration of the moments. This difference in ZFC and FC magnetization decreases with the increase in LNO spacer thickness.

Based on the data of fig. 1 through fig. 5 and earlier studies on ultrathin films of $La_{0.7}Ca_{0.3}MnO_3$ and $LaNiO_3$, a fairly consistent picture of interlayer coupling and magneto-transport emerges in LCMO/LNO superlattices. For LNO layer thickness < 2 u.c. modeling of transport [8] and the behavior of FC/ZFC magnetization suggest a disordered LCMO/LNO interface with thickness ≈ 4 u.c. and frustrated Mn^{3+}, Mn^{4+} and Ni^{3+} spins. We suspect

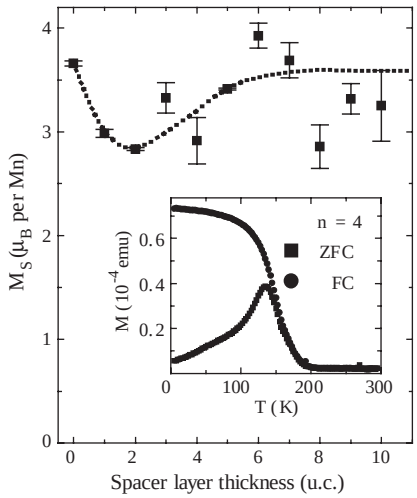

Fig. 5 – LNO spacer layer thickness dependence of the saturation moment per Mn ion in the superlattices. The dotted line in the figure is a guide to the eye and the error bars reflect the uncertainty in the measurements of sample area, which was different for each sample. The inset shows typical zero-field–cooled and field-cooled magnetization curves of the $n = 4$ sample measured at 100 gauss.

that an RKKY-type interaction through this spin-disordered phase causes the AF coupling of the LCMO layers. The steep increase in MR of these multilayers up to a critical field $H_s{}^*$ provides compelling evidence for a correlation between magnetic coupling and transport. The less pronounced but persistent growth of MR with field seen beyond the saturation field is a typical feature of narrow-bandwidth manganites and ultrathin films of even wide-bandwidth systems such as LCMO and LSMO [17, 21–24]. While in the former it is caused by suppression of charge ordering tendencies, in the latter depinning of the magnetic moment (t_{2g} spins) associated with the Mn ions present at the film-substrate interface by the external field is understood to be responsible for the large negative MR. The depinning of the t_{2g} spins at the LCMO-LNO interfaces is arguably a plausible scenario in the present case as well for the persistent growth of MR as seen in fig. 4. It is evident from the sudden drop of the 4 tesla MR in samples with $n < 4$ seen at lower temperatures ($T < 20\,\mathrm{K}$), where limited thermal energy of the localized spins requires much stronger fields for parallel alignment. The freezing/pinning of spins is also evident in the ZFC-FC magnetization data.

At the higher LNO thicknesses, the IEC turns ferromagnetic and the MR does not show a steep increase with the field. Nevertheless, a gradual increase of MR up to the maximum field used in these experiments again points towards pinning of the site spins by interfacial disorder. However, this effect is expected to be less remarkable as the LNO layers gain their bulk-like conductivity and itinerant electrons facilitate coupling of the localized spins. Some indication of this effect comes from the gain in saturation moment and Curie temperature of the multilayers at the higher LNO spacer thicknesses. Finally, the disorder at the interfaces and in the LNO layers is expected to attenuate the oscillatory coupling [25, 26]. The overdamped IEC seen in fig. 2 is consistent with this picture of magnetic ordering in artificial superlattices.

In summary, we have carried out a systematic study to identify the correlation between interlayer exchange coupling and magnetoresistance in superlattices consisting of two metallic oxides one of which is a double-exchange ferromagnet of considerable current interest. We observe overdamped oscillations in the magnetic coupling with the increasing LNO spacer layer thickness. While all multilayers show negative magnetoresistance, the effect is particularly

large in samples where the IEC appears antiferromagnetic. These measurements also suggest that interfacial disorder of magnetic and structural origin plays a much greater role in the behavior of MR than the nature of interlayer magnetic coupling.

* * *

This research has been supported by a grant from the Science and Engineering Research Council of the Department of Science and Technology, Government of India.

REFERENCES

[1] Parkin S. S. P., More N. and Roche K. P., *Phys. Rev. Lett.*, **64** (1990) 2304.
[2] Fert A. and Bruno P., in *Ultrathin Magnetic Structures II*, edited by Heinrich B. and Bland J. A. C. (Springer Verlag, Berlin) 1994, pp. 82-106.
[3] Yafet Y., *Phys. Rev. B*, **36** (1987) 3948.
[4] Bruno P. and Chappert C., *Phys. Rev. Lett.*, **67** (1991) 1602.
[5] Orozco A., Ogale S. B., Li Y. H., Fournier P., Eric Li, Asano H., Smolyaninova V., Greene R. L., Sharma R. P., Ramesh R. and Venkatesan T., *Phys. Rev. Lett.*, **83** (1999) 1680.
[6] Nikolaev K. R., Dobin A. Yu., Krivorotov I. N., Cooly W. K., Bhattacharya A., Kobrinskii A. L., Glazman L. I., Wentzovitch R. M., Dan Dahlberg E. and Goldman A. M., *Phys. Rev. Lett.*, **85** (2000) 3728; Nikolaev K. R., Bhattacharya A., Kraus P. A., Vas'ko V. A., Cooley W. K. and Goldman A. M., *Appl. Phys. Lett.*, **75** (1999) 118.
[7] Parkin S. S. P., *Phys. Rev. Lett.*, **67** (1991) 3598.
[8] Padhan P. and Budhani R. C., *Phys. Rev. B*, **67** (2003) 024414.
[9] Gong G. Q., Gupta A., Gang Xiao, Lecoeur P. and Mcguire T. R., *Phys. Rev. B*, **54** (1996) 3742.
[10] Kwon C., Kim K.-C., Robson M. C., Gu J. Y., Rajeswari M., Venkatesan T. and Ramesh R., *J. Appl. Phys.*, **81** (1997) 4950.
[11] Panagiotopoulos I., Christides C., Pissas M. and Niarchos D., *Phys. Rev. B*, **60** (1999) 485.
[12] Moon-Ho Jo, Neil D. Mathur, Jan E. Evetts, Mark G. Blamire, Manuel Bibes and Josep Fontcuberta, *Appl. Phys. Lett.*, **75** (1999) 3689.
[13] Izumi M., Murakami Y., Konishi Y., Manako T., Kawasaki M. and Tokura Y., *Phys. Rev. B*, **60** (1999) 1211.
[14] Venimadhav A., Hegde M. S., Rawat R., Das I., Paulose P. L. and Sampathkumaran E. V., *Phys. Rev. B*, **63** (2001) 214404.
[15] Jakob G., Moshchalkov V. V. and Bruynseraede Y., *Appl. Phys. Lett.*, **66** (1995) 2464.
[16] Triscone J.-M. and Fischer Ø., *Rep. Prog. Phys.*, **60** (1997) 1673.
[17] Padhan P., Pandey N. K., Srivastava S., Rakshit R. K., Kulkarni V. N. and Budhani R. C., *Solid State Commun.*, **117** (2001) 27.
[18] Barnas J., *J. Magn. & Magn. Mater.*, **111** (1992) L215.
[19] Mattson J. E., Sowers C. H., Berger A. and Bader S. D., *Phys. Rev. Lett.*, **68** (1992) 3252.
[20] Parkin S. S. P., *Phys. Rev. Lett.*, **71** (1993) 1641.
[21] Tokura Y. and Tomioka Y., *J. Magn. & Magn. Mater.*, **200** (1999) 1.
[22] Amlan Biswas, Rajeswari M., Srivastava R. C., Venkatesan T., Greene R. L., Lu Q., Lazanne A. L. and Millis A. J., *Phys. Rev. B*, **63** (2001) 184424.
[23] Fäth M., Freisem S., Menovsky A. A., Tomioka Y., Aarts J. and Mydosh J. A., *Science*, **285** (1999) 1540.
[24] Sun J. Z., Abraham D. W., Rao R. A. and Eom C. B., *Appl. Phys. Lett.*, **74** (1999) 3017.
[25] Bruno P., *Phys. Rev. B*, **52** (1995) 411.
[26] Levy P. M., Sadamichi Maekawa and Bruno P., *Phys. Rev. B*, **58** (1998) 5588.